

Molecular and Electrochemical Impedance Spectroscopic Characterization of the Carbopol Based Bigel and Its Application in Iontophoretic Delivery of Antimicrobials

Vinay K. Singh¹, Arfat Anis², S.M. Al-Zahrani², Dillip K. Pradhan³, Kunal Pal^{1,*}

¹ Department of Biotechnology & Medical Engineering, National Institute of Technology, Rourkela-769008, Odisha, India.

² Department of Chemical Engineering, King Saud University, Riyadh-11421, Saudi Arabia

³ Department of Physics, National Institute of Technology, Rourkela-769008, Odisha, India.

*E-mail: pal.kunal@yahoo.com

Received: 24 April 2014 / Accepted: 15 May 2014 / Published: 16 June 2014

The current study describes development and characterization of carbopol based bigels for the iontophoretic delivery of antimicrobials. The bigels were prepared by mixing carbopol aquagel and sorbitan monostearate (SMS)-sesame oil based oleogels. The molecular characterization of the gels was done by Fourier Transform Infrared (FTIR) spectroscopy and reflectance spectroscopy. The electrical properties were investigated by impedance spectroscopy. Metronidazole (model antimicrobial) loaded bigels were evaluated for their iontophoretic delivery application. FTIR spectra suggested formation of intra/intermolecular hydrogen bonding amongst the gel components. Reflectance spectroscopy showed higher depth of absorption in the bigels containing higher amount of aquagel. The bigels were electro-conductive in nature. The gels containing higher oleogel composition, showed higher bulk resistance and lower drug release. The iontophoretic delivery study showed 13-38% increase in the release of metronidazole under the influence of constant current source. The drug release study of the gels suggested that the gels can be used as matrices for iontophoretic drug delivery applications.

Keywords: bigels, aquagel, oleogel, impedance spectroscopy, iontophoretic delivery.

1. INTRODUCTION

Iontophoresis is a noninvasive technique which employs electric current as stimuli to enhance the penetration of the bioactive agent into the systemic circulation. It enables a targeted delivery of the medicament for the treatment of local conditions (dermatological, ophthalmic or cosmeceuticals) by

topical application. The drug molecule diffuses from the formulations at a faster rate compared to the normal drug delivery due to the synergistic effect of electric current. The rate of release of the drug can be modulated /controlled by altering the applied electric field.

Iontophoresis possess various advantages over the conventional drug delivery system, like reduced systemic side effects and the increased drug penetration directly into the desired site. Hence iontophoresis is getting extensive clinical use in the field of transdermal (local anesthetics, antibiotics) and ocular application (antibacterial, antiviral, and antifungal) of several pharmaceuticals.

Generally, the increased rate of drug release from iontophoresis can be explained by the following mechanisms: (a) enhanced movement of ionic species by the applied electric field, (b) electroosmotic transport of both neutral and charged solute flux within the membrane, (c) electrophoretic transport of solute flux within the membrane and (d) increase in the effective pore radius and permeability by electrically induced swelling of the membrane. *Gratieri et al.* (2013) investigated the iontophoretic delivery kinetics of ketorolac for the treatment of localized inflammation and pain [1].

Bigels are novel gels consisting both aqueous gel and oleogel together in different proportions. As the name suggests, aqueous gels consists of a polar phase as continuous phase whereas the oleogel possess oil continuum phase. Bigels are not emulsions as they do not require emulsifying agent to stabilize the structure [2]. The stability of the bigels is better than those of aqueous gels and oleogels due to the formation of extra-fine dispersion. In recent years, bigels have been the preferred choice of many scientists for pharmaceutical and cosmetic applications.

Carbopol 934 [prop-2-enoic acid, $(C_3H_4O_2)_x$] is a mucoadhesive, biodegradable and environmentally responsive cross-linked acrylic acid polymer [3]. It provides excellent stability and is used to produce opaque gels, emulsions, creams and suspensions for topical application. Sorbitan monostearate [(2R)-2-[(2R,3R,4S)-3,4-dihydroxyoxolan-2-yl]-2-hydroxyethyl octadecanoate, $C_{24}H_{46}O_6$] is an ester of natural fatty acid (stearic acid) and the sugar alcohol sorbitol [4]. It is popularly used as an emulsifying agent and solubiliser in many pharmaceutical and cosmetic products [5].

In this study, iontophoresis was used to deliver the antimicrobials from the bigel system. The bigels were characterized by FTIR spectroscopy, reflectance spectroscopy and impedance spectroscopy. Metronidazole [2-Methyl-5-nitroimidazole-1-ethanol, $C_6H_9N_3O_3$] is a commonly used nitroimidazole derivative with antibacterial property [6]. Metronidazole loaded bigels were evaluated for their iontophoretic delivery application.

2. MATERIALS AND METHODS

2.1. Materials

Carbopol 934 used for the preparation carbopol aquagel and SMS used for the preparation of oleogel were procured from Loba Chemie Pvt. Ltd., Mumbai, India. Food grade sesame oil (Tilsona[®]) was purchased from Recon Oil Industries Pvt. Ltd., Mumbai, India which was used as the organic

phase to prepare the oleogel. Metronidazole (model antimicrobial drug) used to evaluate the iontophoretic drug delivery was provided in-kind by Aarti drugs, Mumbai, India. Double distilled water was used throughout the experiments.

2.2. Methods

2.2.1. Preparation of bigels

Carbopol aquagel was prepared by dissolving required quantities of carbopol (1% w/w) in warm water maintained at 60 °C which was kept on stirring at 500 rpm. The stirring was continued until a homogenous mixture was obtained.

SMS-sesame oil oleogel was prepared by dissolving accurately weighed SMS (15% w/w) in sesame oil maintained at 60 °C, which was kept on stirring at 500 rpm. The hot mixture was subsequently cooled to room-temperature (25 °C).

The bigels were prepared by mixing the oleogel and aquagel maintained at 60 °C. The specified quantities of molten oleogel were added drop-wise in the hot carbopol aquagel (60 °C, 500 rpm) (Table 1). The stirring was continued for 30 min at the same experimental conditions. The hot mixture was cooled down to room temperature. Metronidazole (model antimicrobial drugs) was loaded in the oleogel. The method of preparation remained same except that the sufficient amount of metronidazole was uniformly dispersed in sesame oil before adding SMS. The loading amount of metronidazole was kept constant (1 % w/w) in all the bigels.

2.2.2. Molecular properties

The molecular properties of the prepared bigels were studied using Fourier Transform Infrared (FTIR) spectroscopy and reflectance spectroscopy. FTIR spectroscopy was performed using Bruker ALPHA-E FTIR spectrophotometer (USA) being operated in the Attenuated Total Reflectance (ATR) mode in the wavenumber range of 4000 to 500 cm^{-1} [7].

The absorbance behavior of the developed bigels in the UV-visible region was studied using UV/Vis spectrophotometer (Lambda 35 UV/Vis spectrophotometer, Perkin Elmer, USA) [8].

2.2.3. Electrochemical impedance spectroscopy

The electrical properties of the bigels were studied using computer controlled impedance analyzer (Phase sensitive multimeter, PSM1735, Numetriq, Japan) The impedance parameters such as impedance, phase angle, capacitance and loss tangent were measured using copper electrodes [9].

2.2.4. Iontophoretic drug delivery

Iontophoretic drug delivery is based on the principle of drug release under the influence of electric current. The *in vitro* drug release studies (active and passive form) were performed using an in-house developed iontophoretic drug delivery setup. Accurately weighed (~2.15 g) metronidazole loaded gels were kept in the donor compartment, and a previously activated dialysis membrane (MW cut-off - 60 kDa, Himedia, Mumbai) was tied at one end. The receptor compartment contained 25 ml distilled water which was kept on stirring at 100 rpm maintained at 37 °C to simulate the physiological conditions. Stainless steel electrodes (diameter 1.4 cm) were connected to the donor and the receptor chambers. The study was conducted using an a.c. current of 32.13 μA (I_{rms}), which provided a current density of 20.88 $\mu\text{A}/\text{cm}^2$. The voltage controlled constant current source was developed using a standard signal generator which generated a sinusoidal voltage of 0.707 V (V_{rms}). 3 ml of the releasate was collected at regular intervals (0.25, 0.5, 0.75, 1, 1.5 and 2h). 3 ml of fresh water was subsequently added to the receptor compartment to maintain the volume of the dissolution media to 25 ml. The absorbances of the releasate were noted using a UV-vis spectrophotometer (UV 3200 double beam, Labindia) at 321 nm and the cumulative percent drug release was calculated [10-11].

3. RESULTS AND DISCUSSION

3.1. Preparation of bigels

The carbopol aquagel was homogenous and yellowish white in color. The SMS-sesame oil oleogel was smooth, slightly yellowish clear hot mixture which turned into turbid gel when cooled down to room temperature. The formation of gel was confirmed by inverting the container in which the gels were prepared. The oleogel was smooth in texture and oily to touch. When SMS-sesame oil oleogel was added in the carbopol aquagel dropwise, a milky white homogenous viscous mixture was obtained. The homogenous mixture at room-temperature was converted into gel (Table 1). The bigels had a smooth texture and were milky white in color. F1 and F2 were easy spreading and were less sticky in nature. F3 and F4 showed better spreadability and were very sticky in nature. The consistency, smoothness and stickiness of the bigels increased linearly with increase in oleogel content. The bigels containing higher oleogel content showed quicker gel formation.

Table 1. Compositions of bigel formulations (% w/w)

Formulations	Carbopol aquagel	Oleogel	Metronidazole
F1	88.89	11.11	-
F1M	88.89	10.11	1
F2	80	20	-
F2M	80	19	1
F3	72.73	27.27	-
F3M	72.73	26.27	1
F4	66.67	33.33	-
F4M	66.67	32.33	1

3.2. Molecular properties

The molecular integrity, compatibility and interactions amongst the gel components (polymers, oil, SMS and drug) were evaluated with the help of FTIR spectroscopy (Figure 1a). The absorption peak at $\sim 3300\text{ cm}^{-1}$ was associated to the O-H stretching vibration (carbopol, SMS and sesame oil) [12]. The peaks at $\sim 2800\text{ cm}^{-1}$ was due to the C-H stretching vibration of alkanes (SMS and sesame oil). The absorption peak at $\sim 1758\text{ cm}^{-1}$ was due to C=O stretching vibration (carbopol, SMS and sesame oil) [13]. The absorption band at $\sim 1650\text{ cm}^{-1}$ (carbopol) and at $\sim 1465\text{ cm}^{-1}$ (carbopol, SMS and sesame oil) was due to (O-C-O) asymmetric and symmetric stretching vibrations, respectively [14]. A prominent peak at $\sim 1160\text{ cm}^{-1}$ represented a stretching vibration of C-O-C ethereal group (carbopol) [15]. The peak at $\sim 1100\text{ cm}^{-1}$ was due to the stretching of the C-F group (carbopol) [16]. All the principle peaks of the raw materials (carbopol, SMS and sesame oil) were present in the blank as well as the metronidazole loaded bigels. This suggested that the formulation components were compatible with each other and did not chemically interact amongst themselves. The FTIR spectra of the bigels showed prominent band at $\sim 3300\text{ cm}^{-1}$, which is assigned to O-H stretching vibrations due to the presence of strong intramolecular/ intermolecular hydrogen bonding. FTIR bands are sharp in case of intramolecular hydrogen bonding, whereas the bands are broad in intermolecular hydrogen bonding [17]. The presence of broad FTIR band suggested formation of intermolecular hydrogen bonding. The extent of intermolecular hydrogen bonding was quantified by calculating the area under the peak ($3700 - 2950\text{ cm}^{-1}$) (Table 2) [18]. The results suggested that the formulations have shown almost similar extent of hydrogen bonding and addition of metronidazole did not affect it significantly. The peaks associated with metronidazole were not observed in the bigels due to very low concentrations of metronidazole.

Table 2. AUC for the peak at $\sim 3300\text{ cm}^{-1}$ ($3700 - 2950\text{ cm}^{-1}$)

Formulations	AUC
F1	1194.41
F1M	1169.49
F2	1159.2
F2M	1163.14
F3	1176.41
F3M	1191.76
F4	1182.02
F4M	1065.67

Diffuse reflectance is a non-linear process, associated with the drop in reflection at certain points in the spectrum. The drop in the spectrum is due to the absorbed light by electrons. A typical reflectance spectrum of the developed bigels is shown in Figure 1b where the percent reflectance is plotted as a function of wavelength. The points of appearance of dips are characteristic of certain ions,

molecules, and minerals. The apparent depth (D) of absorption, relative to the surrounding continuum in a reflectance spectrum is given by equation:

$$D = 1 - R_b/R_c \tag{1}$$

where R_b and R_c are the reflectance at the bottom of the band and the reflectance of the continuum at the same wavelength as R_b [19].

The depth of absorption band was in the order $F1 > F2 > F3 > F4 > C934$ (Figure 1b inset). The results correlate to the droplet size as determined from the bright field microscopy not reported here. The decrease in the droplet size of the dispersed globules showed more scattering causing a decrease in the strength of all the absorptions, thus, decreasing the spectral sensitivity to carbopol 934 content in the formulations.

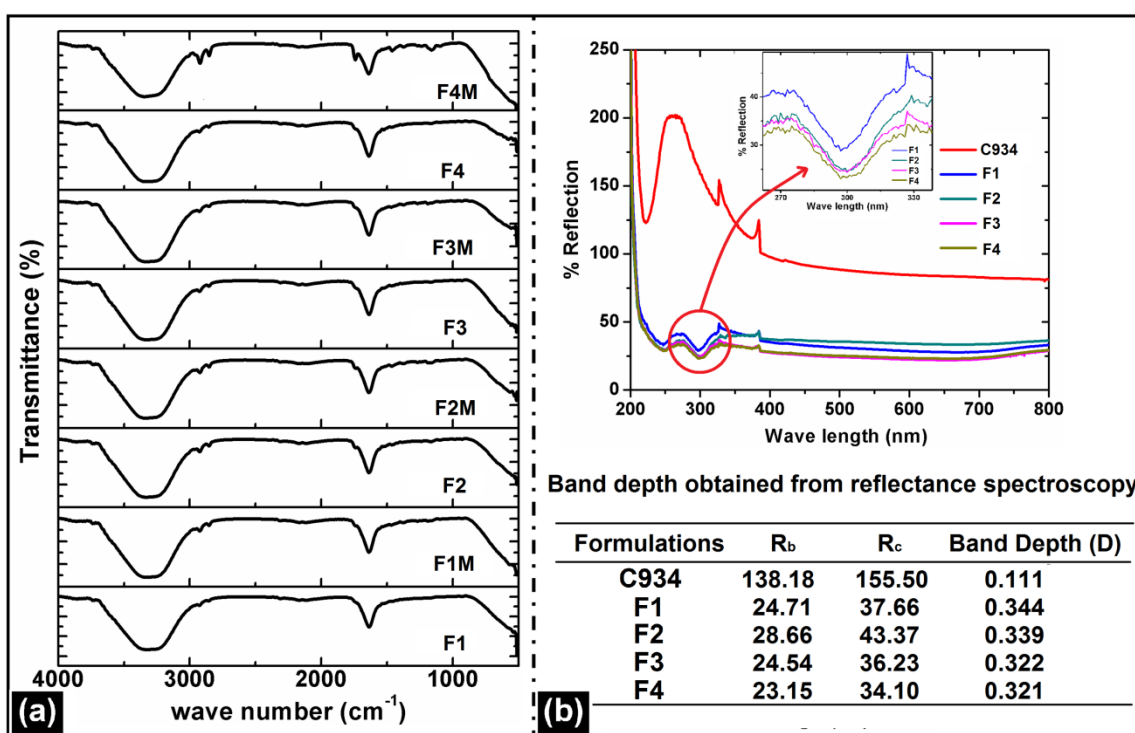


Figure 1. Molecular properties of the bigels (a) FTIR spectroscopy and (b) Diffuse reflectance spectroscopy.

3.3. Electrical properties

The impedance spectroscopy study was performed to study the electrical transport behavior of the bigels. In order to observe the effect of smallest capacitance and the largest resistance, it is necessary to plot impedance (Z'') and modulus (M'') spectroscopic plots versus frequency simultaneously [20]. Figure 2a shows the impedance (Z'') and modulus (M'') spectroscopic plots at room-temperature. Two peaks were observed for all the bigels, one corresponding to the grain (high frequency) and another to the grain boundary (low frequency) [21]. The peaks were well resolved and indicated the presence of both the grain and interface relaxation phenomena in the bigels. The peaks

were broadened in the low frequency region whereas these were sharp in the higher frequency region. The asymmetric peak broadening is related to the spread of relaxation times. The sharp peaks in high frequency region suggested shorter relaxation times and higher conductivity. The peak positions of Z'' and M'' in spectroscopic plots were slightly separated from each other suggesting a non-Debye behavior and justify the presence of a constant phase element (CPE) in the equivalent circuit diagram. The mismatch of peak positions can be attributed to the presence of localized movement of the charge carriers.

Complex impedance spectra (Nyquist plot, $-Z''$ vs. Z') of the bigels have been shown in [Figure 2b](#). The plots exhibited two well-defined regions, namely, a high frequency region semicircle and a non-vertical spike at lower frequency. The formation of high frequency semicircle can be attributed to the bulk effect of electrolytes whereas the non-vertical spike is associated to the roughness of the electrode-electrolyte interface [22].

The bulk resistance (R_b) of the formulations was obtained from the intersection of the high frequency impedance semicircle with the real axis (Z'). The bulk resistance of the formulations was higher in formulations with higher proportions of oleogels. Since oleogels are non-conducting, the impedance of the bigels was mainly due to the oleogels. The formation of electrical double layer can be explained by the CPE which varies based on the microstructure of the bigels. Hence the information about the microstructure can be gathered using the CPE element.

The complete analysis of the electrical property of the bigels was done by modelling an electrical equivalent circuit. The bulk resistance and the bulk capacitance, obtained from the Nyquist plot, are connected in parallel and the spike is represented by a double-layer capacitance which is connected in series [22]. The inhomogeneity of the system is compensated by adding a CPE element in the equivalent circuit. Two constant phase elements have been introduced in the equivalent circuit named as CPE1 and CPE2. CPE1 represents the double-layer capacitance between the electrode–bigels interface whereas the bulk effects are represented by CPE2. The semicircle obtained in high-frequency region was due to the parallel combination of bulk resistance, bulk capacitance and CPE2, whereas the non-vertical spike can be explained with CPE1. The impedance spectrum was fitted by the above equivalent circuit, using commercially available computer software Z SimpWin. The fitted lines are shown in red ([Figure 2b](#)), indicating a good fit. The impedance data was fitted to the equivalent circuit and parameters such as bulk resistance and bulk capacitance were tabulated in [Table 3](#).

[Figure 2c](#) shows the variation in the conductivity (σ_{ac}) of the bigels as a function of frequency. The conductivity profile showed three zones; a low frequency dependent dispersion region, an intermediate frequency plateau region and a high frequency dispersion region [23]. The low frequency dispersion region is attributed to space charge polarization at the material electrode interface [24]. The frequency independent plateau region is associated with the bulk conductivity of the bigels, whereas the high frequency dispersion region is due to the a.c. conductivity of the materials.

The frequency dependence of the conductivity can be best expressed by Jonscher power law given by the following equation.

$$\sigma_{ac} = \sigma_0 + A\omega^s \quad (2)$$

where, σ_{ac} is a.c. conductivity; σ_0 is d.c. conductivity; A is a pre-exponential constant; $\omega = 2\pi f$ is angular frequency and s is power law exponent, where $0 < s < 1$ [18].

The conductivity of the bigels was in the order of F1> F2> F3> F4. The conductivity of the gels decreased monotonically with increased proportion of the oleogel in the bigels. The increase in the non-conducting element (oleogel) resulted in the decrease in conductivity of the bigels. The d.c. conductivity of the bigels was calculated using the formula:

$$\sigma_0 = (1/R_b) * (l/A) \tag{3}$$

Where, l is the thickness and A is the area of the sample. The d.c. conductivity of the gels was in the same order as the a.c. conductivity (F1> F2> F3> F4) (Table 3).

Table 3. Electrical properties of the bigels

Formulations	R _b (10 ³)	C _b (10 ⁻¹¹)	σ _{dc}
F1	5.562	4.54	0.229
F2	8.707	5.50	0.146
F3	15.1	4.90	0.084
F4	19.7	4.92	0.064

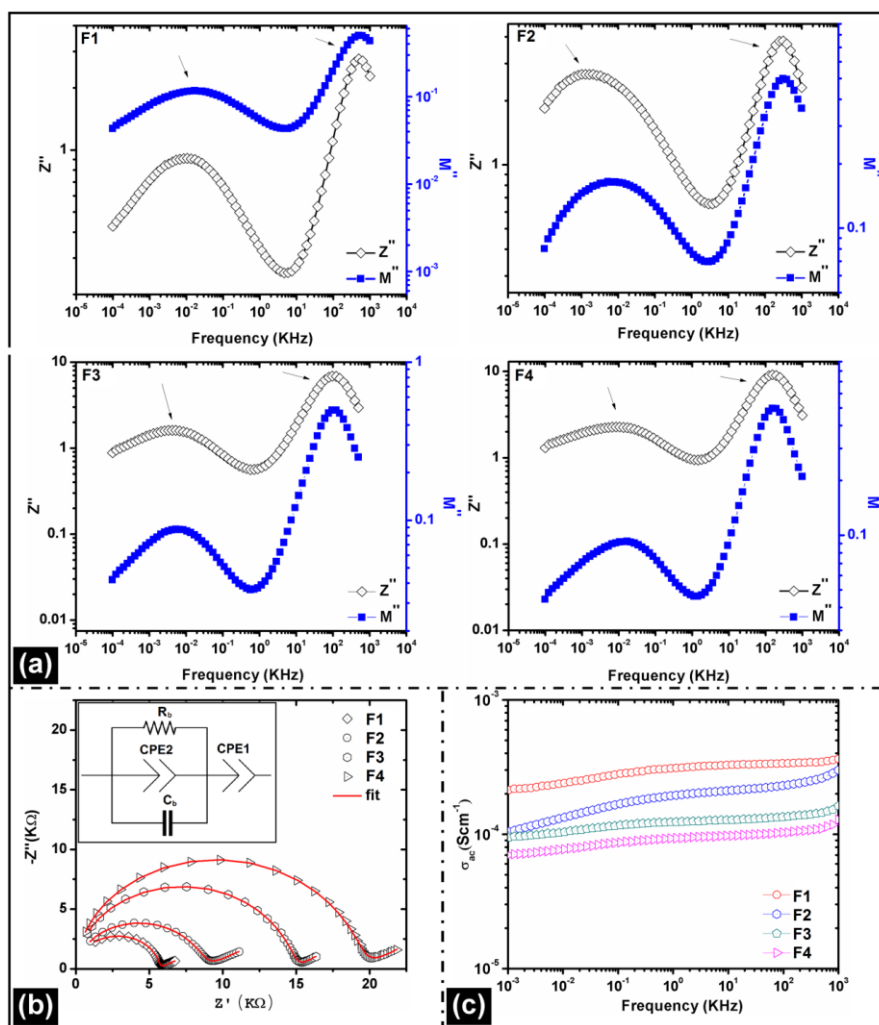


Figure 2. Electrical properties of the bigels (a) impedance (Z'') and modulus (M'') spectroscopic plots, (b) Nyquist plot and (c) a.c. conductivity.

3.4. Iontophoretic drug delivery

The bigels showed highly conductive nature as observed in impedance spectroscopy. The conductive nature of the gels should help in improving the release rate of the drugs from the formulations. Keeping these facts in the mind, the metronidazole loaded bigels were tested as possible matrices for their iontophoretic drug delivery applications. The drug release using iontophoresis involves release of the drug based on application of an electric field onto the charged drug molecules [25-26]. The preliminary experimentations showed the release of metronidazole from the bigels was in the order $F1 > F2 > F3 > F4$ in both active and passive conditions (Figure 3 a-b). The amount of water present in the gels played a major role. The gels containing higher water concentrations showed higher release of metronidazole from the gel matrix. The rate of release of drug was higher in active condition compared to the passive conditions which suggested that the presence of electrical field increased the release rate of the drug.

The percent increase in the released drug was highest in F1M (~38) and was lowest in F4M (~13.5) over a period of 2 h (Figure 3c). The gels containing higher aqueous component showed higher increase in percent drug release. It was in the order $F1 > F2 \geq F3 > F4$. Metronidazole showed higher partitioning from the gels into the dissolution medium (water) when the concentration of water was higher in F1M. A significant increase in percent drug release was observed in all the bigels in the presence of externally applied electrical field. The bigels containing higher aqueous proportion showed higher increase in percent drug release. Hence it can be concluded that the developed bigels can be used as carriers for iontophoretic drug delivery [27].

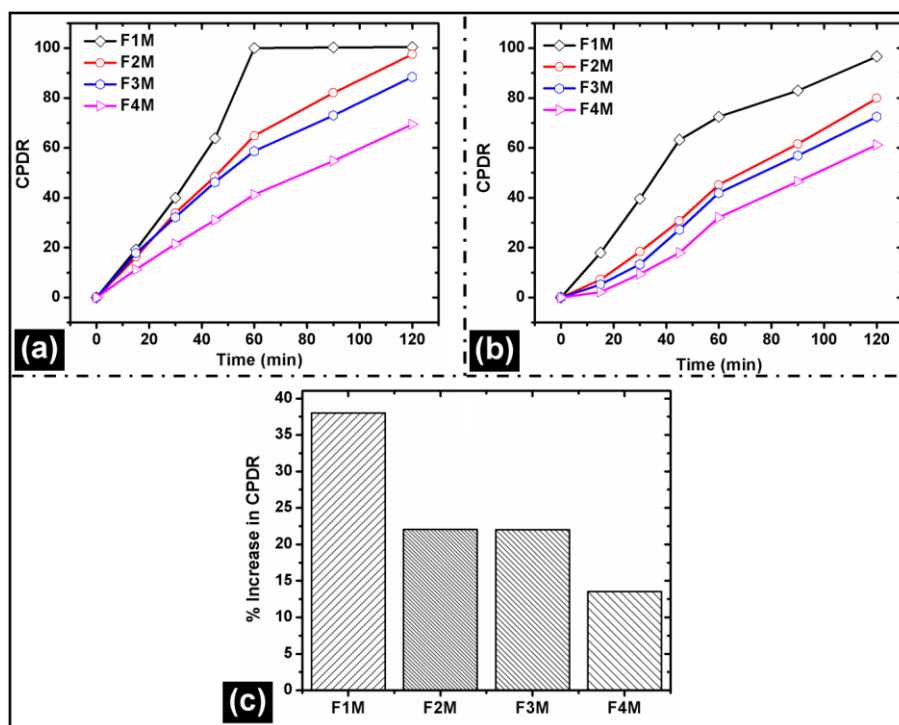


Figure 3. In-vitro drug release, Cumulative percent drug release (a) active release (b) passive release (c) Percent increase in drug release.

The release kinetics of the drug release was studied by applying various kinetic models. The results showed that the release of metronidazole from the bigels followed zero-order kinetics thereby suggesting concentration independent release behavior (Figure 4a). Korsmeyer-Peppas model was fitted to check the diffusion coefficient (n) value (Figure 4b). The n-value was found to be in between 0.85 and 1.16 for all the bigels suggesting non-Fickian diffusion of metronidazole [28]. In general, non-Fickian diffusion is followed when the release mechanism is not well known or when more than one mechanisms are involved. The possible mechanism may be swelling and diffusion mediated release [29].

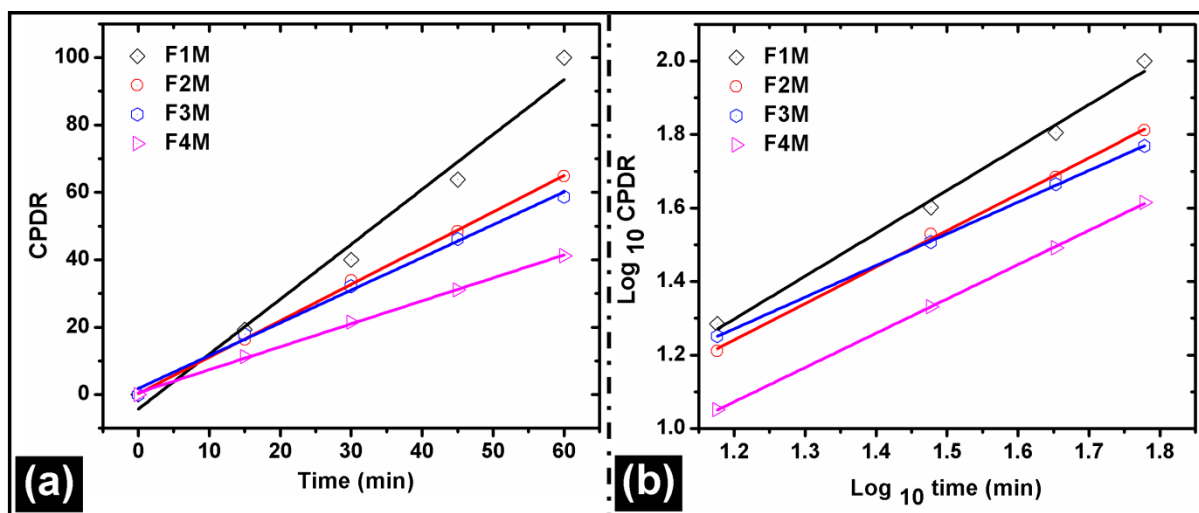


Figure 4. Drug release kinetic (a) zero order fitting and (b) KP model fitting.

Table 4. Drug release study of the developed bigels

Formulations	F1M	F2M	F3M	F4M
CPDR				
Active	99.97±4.22	97.46±3.65	88.44±2.84	69.42±2.61
Passive	96.62±4.37	79.86±3.62	72.49±3.73	61.15±2.78
Drug release kinetics				
Zero order				
Adj.R-Square	0.976	0.999	0.994	0.999
KP Model				
Adj. R-Square	0.990	0.997	0.999	0.999
n-value	1.16	0.99	0.86	0.93

The n-value was found to be < 1 for all the bigels except F1M, suggesting case-II diffusion transport mechanism. Case-II transport mechanism has been associated with the zero order release [28]. The n-value obtained in F1M was 1.16, which indicated super case-II transport of drug from the gel. In super case-II transport mechanism, two kinds of fluxes exist simultaneously during the drug

delivery [30]. During the first flux, the drug diffuses at the polymer interface by polymer relaxation. During the second flux, drug diffuses away from the interface.

4. CONCLUSION

The study successfully explained the development of carbopol 934 based bigels which can be used as matrices for iontophoretic drug delivery. The method of preparation was easy and economical. The bigels were smooth and easily spreadable. Metronidazole (model antimicrobial) loaded bigels were evaluated for their iontophoretic delivery application. The bigels showed good conductivity which was dependent on the oleogel concentration. The conductivity and percent metronidazole release from the bigel showed linear decrease with increase in oleogel content. A considerable percent increase in the release of metronidazole was observed when drug release was conducted under a constant current source. The observed properties render the developed bigels as promising matrices for iontophoretic drug delivery applications. The release of the drug can be modulated/controlled in a predictable manner by altering the composition of the bigel.

ACKNOWLEDGEMENT

Authors acknowledge the support provided by National Institute of Technology, Rourkela for the completion of this study. The authors would like to extend their sincere appreciation to the Deanship of Scientific Research at King Saud University for its funding of this research through the Research Group Project No. RGP-VPP-095.

References

1. T. Gratieri, E. Pujol-Bello, G. M. Gelfuso, J. G. de Souza, R. F. Lopez, and Y. N. Kalia, *Eur J Pharm Biopharm*, 86 (2013) 219.
2. L. Di Michele, F. Varrato, D. Fiocco, S. Sastry, E. Eiser, and G. Foffi, *Soft Matter*, 10 (2014) 3633.
3. K. V. Nikumbh, S. G. Sevankar, and M. P. Patil, *Drug Deliv*, (2013) 1. (doi: 10.3109/10717544.2013.859186)
4. Q. Zhao, W. Kuang, Z. Long, M. Fang, D. Liu, B. Yang, and M. Zhao, *Food chem*, 141 (2013) 1834.
5. S. Sahoo, N. Kumar, C. Bhattacharya, S. Sagiri, K. Jain, K. Pal, S. Ray, and B. Nayak, *Des Monomers Polym*, 14 (2011) 95.
6. Z. Fang, J. Chen, X. Qiu, X. Qiu, W. Cheng, and L. Zhu, *Desalination*, 268 (2011) 60.
7. S. Sahoo, C. Chakraborti, S. Naik, S. Mishra, and U. Nanda, *Trop J Pharm Res*, 10 (2011) 273.
8. S. Chin, E. Park, M. Kim, G.-N. Bae, and J. Jurng, *Mater Lett*, 75 (2012) 57.
9. S. Pradhan, S. S. Sagiri, V. K. Singh, K. Pal, S. S. Ray, and D. K. Pradhan, *J Appl Polym Sci*, 131 (2014) (doi: 10.1002/app.39979)
10. V. Vamathevan, R. Amal, D. Beydoun, G. Low, and S. McEvoy, *J Photoch Photobio C*, 148 (2002) 233.
11. K. Pal, A. Bantia, and D. Majumdar, *AAPS PharmSciTech*, 8 (2007) E142.
12. S. Ifuku, Y. Tsujii, H. Kamitakahara, T. Takano, and F. Nakatsubo, *J Polym Sci A Polym Chem*, 43 (2005) 5023.

13. C. Schild, A. Wokaun, and A. Baiker, *J Mol Catal*, 63 (1990) 223.
14. J. Desai, K. Alexander, and A. Riga, *Int J Pharm*, 308 (2006) 115.
15. E. Bilensoy, Y. Cırpanlı, M. Şen, A. L. Doğan, and S. Çalış, *J Incl Phenom Macro*, 57 (2007) 363.
16. V. K. Singh, K. Pal, D. K. Pradhan, and K. Pramanik, *J Appl Polym Sci*, 130 (2013) 1503.
17. D. Satapathy, D. Biswas, B. Behera, S. Sagiri, K. Pal, and K. Pramanik, *J Appl Polym Sci*, 129 (2013) 585.
18. V. K. Singh, S. Ramesh, K. Pal, A. Anis, D. K. Pradhan, and K. Pramanik, *J Mater Sci Mater Med*, 25 (2013) 703.
19. R. N. Clark, *Manual of remote sensing*, 3 (1999) 3.
20. B. Barick, K. Mishra, A. Arora, R. Choudhary, and D. K. Pradhan, *J Phys D Appl Phys*, 44 (2011) 355402.
21. S. C. Hwang, and G. M. Choi, *Solid State Ionics*, 179 (2008) 1042.
22. D. K. Pradhan, R. Choudhary, B. Samantaray, A. K. Thakur, and R. Katiyar, *Ionics*, 15 (2009) 345.
23. D. K. Pradhan, R. Choudhary, and B. Samantaray, *Express Polym Lett*, 2 (2008) 630.
24. D. K. Pradhan, B. Samantaray, R. Choudhary, and A. K. Thakur, *J Mater Sci-Mater El*, 17 (2006) 157.
25. Y. N. Kalia, A. Naik, J. Garrison, and R. H. Guy, *Adv Drug Deliver Rev*, 56 (2004) 619.
26. R. Prasad, V. Koul, S. Anand, and R. Khar, *Int J Pharm*, 333 (2007) 70.
27. J. E. Möckel, and B. C. Lippold, *Pharmaceut Res*, 10 (1993) 1066.
28. S. Dash, P. N. Murthy, L. Nath, and P. Chowdhury, *Acta Pol Pharm*, 67 (2010) 217.
29. J. Varshosaz, M. Tabbakhian, and Z. Salmani, *The Open Drug Delivery J*, 2 (2008) 61.
30. A. Figueiras, A. C. C. Pais, and F. B. Veiga, *AAPS PharmSciTech*, 11 (2010) 1703.